

Formation and Energy Band Engineering of Ternary Alloy $\text{Ge}_{1-x-y}\text{Sn}_x\text{C}_y$ Layers

T. Yamaha¹, H. Oda¹, M. Kurosawa^{1,2}, W. Takeuchi¹, N. Taoka¹, O. Nakatsuka¹, S. Zaima¹

¹Graduate School of Engineering, Nagoya University, Furo-cho, Chikusa-ku, Nagoya 464-8603, Japan

²JSPS Research Fellow, 5-3-1 Kojimachi, Chiyoda-ku, Tokyo 102-0083, Japan

Phone: +81-52-789-3819, FAX: +81-52-789-2760, e-mail: tyamaha@alice.xtal.nagoya-u.ac.jp

Abstract

We have investigated the crystalline and optical properties of epitaxial layers of ternary alloy $\text{Ge}_{1-x-y}\text{Sn}_x\text{C}_y$ grown on Si. We achieved the formation of strain relaxed $\text{Ge}_{1-x-y}\text{Sn}_x\text{C}_y$ epitaxial layers with a C content as high as 2%. XPS and Raman spectroscopy measurements revealed that C atoms preferentially bond with Sn atoms, which enhances the incorporation of C atoms into substitutional sites in Ge. We also demonstrate the control of the energy bandgap of $\text{Ge}_{1-x-y}\text{Sn}_x\text{C}_y$ layers with the Sn content.

1. Introduction

$\text{Ge}_{1-x-y}\text{Sn}_x\text{C}_y$ ternary alloy is one of attractive materials for electronic, optoelectronic, and photovoltaic applications. $\text{Ge}_{1-y}\text{C}_y$ and $\text{Ge}_{1-x}\text{Sn}_x$ with a high C or Sn content over a several % promise to be a direct bandgap semiconductor with group-IV elements [1,2]. In addition, $\text{Ge}_{1-x-y}\text{Sn}_x\text{C}_y$ ternary alloy is expected to realize independent control of the energy band structure and lattice constant with controlling each element content. However, the thermoequilibrium solubility of Sn and C in Ge is very low, below 1% [3,4]. Especially, the substitutional C content in a $\text{Ge}_{1-y}\text{C}_y$ epitaxial layer grown on Si substrate is reported as low as 2.6% even with a flux C content of 7% [5]. On the other hand, the binding energy of Sn-C bond and Sn-vacancy is expected to be stable in Ge matrix by theoretical calculation [6]. Hence, simultaneous incorporation of Sn and C atoms is expected to raise the substitutional C content. In fact, we recently reported that the substitutional C content can be raised by the formation of $\text{Ge}_{1-x-y}\text{Sn}_x\text{C}_y$ ternary alloy layer grown on Ge substrate [7]. However, the relationship between Sn and C in Ge matrix and the optical property of $\text{Ge}_{1-x-y}\text{Sn}_x\text{C}_y$ layers have not been understood in detail yet. In this study, we prepared $\text{Ge}_{1-x-y}\text{Sn}_x\text{C}_y$ epitaxial layers on Si substrate and investigated the crystalline and optical properties of $\text{Ge}_{1-x-y}\text{Sn}_x\text{C}_y$ layers.

2. Sample preparation

After chemically and thermally cleaning Si (001) substrate, a $\text{Ge}_{1-x-y}\text{Sn}_x\text{C}_y$ layer was grown on Si by using a radio frequency (RF) sputtering system. The substrate temperature was 290°C, and the thickness was 200 nm. The content of Sn was ranging from 0% to 8% by controlling the sputtering rate, while the C content was fixed at 2%. The surface cleaning of Si substrate and the epitaxial growth of $\text{Ge}_{1-x-y}\text{Sn}_x\text{C}_y$ layer was confirmed with reflective high-energy electron diffraction (RHEED).

3. Results and discussion

Figure 1(a) shows a typical result of X-ray diffraction two dimensional reciprocal space mapping (XRD-2DRSM) around the $\bar{2}24$ reciprocal lattice point for the $\text{Ge}_{1-x-y}\text{Sn}_x\text{C}_y/\text{Si}$ sample with a Sn content of 3.6%. Figure 1 (b)

shows the summary of the diffraction peak positions of $\text{Ge}_{1-x-y}\text{Sn}_x\text{C}_y$ layers estimated with XRD-2DRSM. We can see that the strain in all $\text{Ge}_{1-x-y}\text{Sn}_x\text{C}_y$ layers on Si is fully relaxed. Also, the lattice constant of $\text{Ge}_{1-x-y}\text{Sn}_x\text{C}_y$ layer can be controlled with the Sn content.

We investigated the chemical bonding state of C in $\text{Ge}_{1-x-y}\text{Sn}_x\text{C}_y$ layers with X-ray photoelectron spectroscopy (XPS). Figures 2(a) and 2(b) show photoelectron spectrum of the C1s bonding state for $\text{Ge}_{0.98}\text{C}_{0.02}$ (without Sn) and $\text{Ge}_{0.90}\text{Sn}_{0.08}\text{C}_{0.02}$ layers, respectively. The C1s spectrum was deconvoluted assuming two kinds of the chemical bonding states related to C-C at 285 eV and C-Ge or C-Sn at 283 eV. We consider that the C-C bond should be related to interstitial or precipitated C atoms. Hence, the substitutional C content in Ge was estimated from the area intensity of the bonding state related C-Ge or C-Sn bond. Figure 3 shows the area intensity of the peaks related to C-C and C-Sn/C-Ge bonds as a function of the Sn content. The area intensity related to the C-C bond obviously decreases with incorporation of Sn, while the total C content is a little fluctuated due to the variability of the deposition condition. The intensity ratio of the bonding state related to C-Ge or C-Sn to the total bonding state is higher than 90% in $\text{Ge}_{1-x-y}\text{Sn}_x\text{C}_y$ with a Sn content of 8.1%.

Figures 4 (a) and 4(b) show Raman scattering spectra related to Ge-Ge and Ge-C bonds, respectively, for the $\text{Ge}_{1-x-y}\text{Sn}_x\text{C}_y/\text{Si}$ samples. The peak related to Ge-Ge bond shifts to a smaller wavenumber with increasing in the substitutional Sn content. On the other hand, the peak related to Ge-C bond is clearly observed around 550 cm^{-1} only for the $\text{Ge}_{1-y}\text{C}_y/\text{Si}$ sample without Sn. Results of XPS and Raman scattering measurements indicate that C atoms in $\text{Ge}_{1-x-y}\text{Sn}_x\text{C}_y$ layer preferentially bonds with Sn atoms, that can be attributed to the compensation of the local strain around Sn and C in Ge matrix.

Figure 5 shows the Tauc plot for indirect transition from the absorption spectrum of $\text{Ge}_{1-x-y}\text{Sn}_x\text{C}_y/\text{Si}$ samples measured with Fourier transform infrared spectroscopy (FTIR). The energy bandgap can be estimated by the following Tauc equation [8],

$$(\alpha h\nu)^{1/n} = (h\nu - E_g) \quad (1)$$

where α is the absorption coefficient, ν is the frequency of incident photon, and E_g is the energy bandgap of $\text{Ge}_{1-x-y}\text{Sn}_x\text{C}_y$ layer. Here, the n value was estimated to be about 2 for all samples, meaning that the indirect transition is dominant. Figure 6 shows the Sn content dependence of the energy bandgap of $\text{Ge}_{1-x-y}\text{Sn}_x\text{C}_y$ layers. Theoretically predicted energy bandgap of $\text{Ge}_{1-x}\text{Sn}_x$ without C is also shown for reference [2]. The energy bandgap of ternary alloy $\text{Ge}_{1-x-y}\text{Sn}_x\text{C}_y$ layers can be controlled from 0.60 eV to 0.55 eV with increasing in the Sn content of 0–8%.

4. Conclusions

We investigated the crystalline and optical properties of strain relaxed $\text{Ge}_{1-x}\text{Sn}_x\text{C}_y$ layers on Si substrate with a C content as high as 2%. The Sn incorporation improves on the introduction of C into substitutional sites in Ge matrix with the formation of Sn-C bond, which would compensate the local strain. We demonstrated the energy band engineering of $\text{Ge}_{1-x}\text{Sn}_x\text{C}_y$ layer with controlling Sn and C contents.

Acknowledgements

This work was partially supported by the ALCA program of JST in Japan.

References

- [1] J. Kolodzey *et al.*, J. Crystal Growth **157** (1995) 386.
- [2] Y. Chibane *et al.*, J. Appl. Phys. **107** (2010) 053512.
- [3] C. D. Thurmond *et al.*, J. Chem. Phys. **25** (1956) 799.
- [4] J. D'Arcy-Gall *et al.*, J. Appl. Phys. **88** (2000) 96.
- [5] M. Okinaka *et al.*, J. Cryst. Growth. **249** (2003) 78.
- [6] A. Chroneos *et al.*, Phys. Stat. sol. (b) **244** 9 (2007) 3206.
- [7] K. Terasawa *et al.*, in *Abstra. of Int. SiGe Tech. Dev. Meeting (ISTDM) 2014*, Singapore, June, 2014.
- [8] J. Tauc *et al.*, Phys. Stat. Sol. **15** (1966) 627.

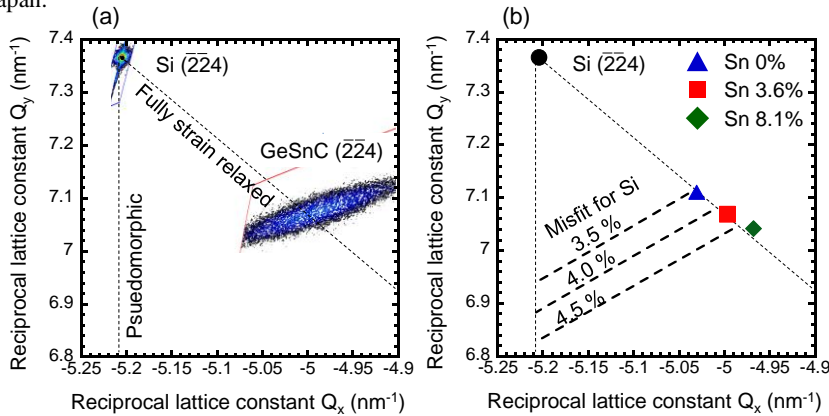


Fig. 1. (a) XRD-2DRSM for the $\text{Ge}_{0.944}\text{Sn}_{0.036}\text{C}_{0.02}/\text{Si}$ sample. (b) Summary of the diffraction positions of $\text{Ge}_{1-x}\text{Sn}_x\text{C}_y$ layers estimated with XRD-2DRSM.

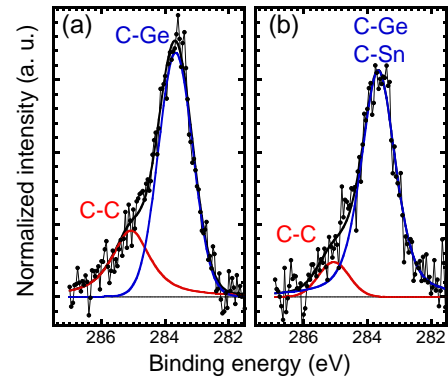


Fig. 2. Photoelectron spectra of C1s bonding state for (a) $\text{Ge}_{0.98}\text{C}_{0.02}$ without Sn and (b) $\text{Ge}_{0.90}\text{Sn}_{0.08}\text{C}_{0.02}$ layers.

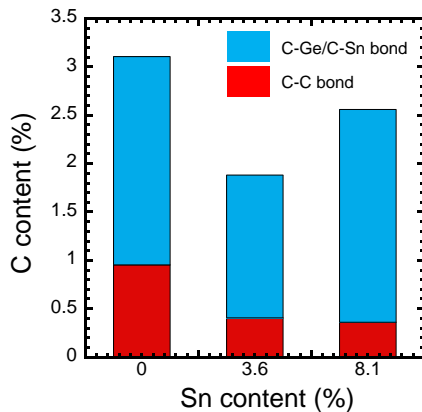


Fig. 3. The area intensity of the peaks related to C-C and C-Sn/C-Ge bonds as a function of the Sn content for the $\text{Ge}_{1-x}\text{Sn}_x\text{C}_y/\text{Si}$ samples.

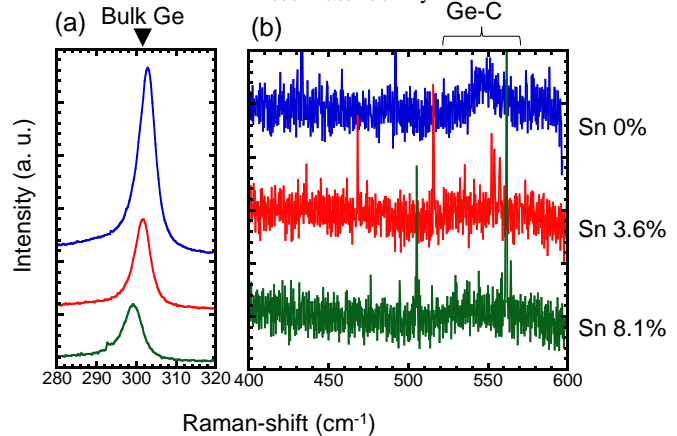


Fig. 4. Raman scattering spectra related to (a) Ge-Ge and (b) Ge-C bonds for the $\text{Ge}_{1-x}\text{Sn}_x\text{C}_y/\text{Si}$ samples.

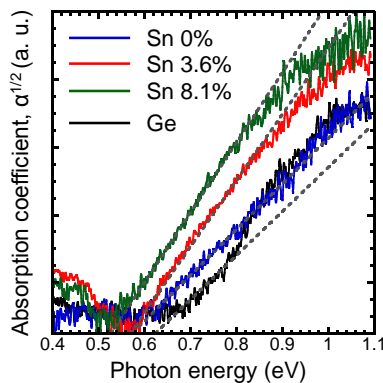


Fig. 5. Indirect Tauc plot obtained FT-IR absorption spectra for the $\text{Ge}_{1-x}\text{Sn}_x\text{C}_y/\text{Si}$ samples and Ge substrate.

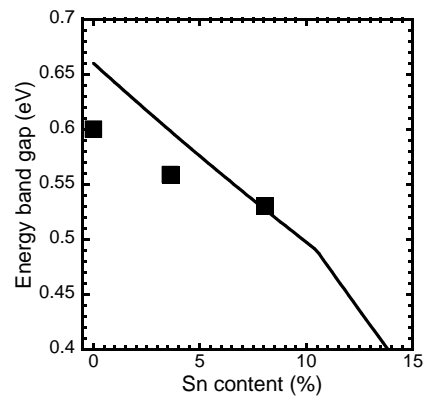


Fig. 6. The Sn content dependence of the energy bandgap for $\text{Ge}_{1-x}\text{Sn}_x\text{C}_y$ layers. Theoretically predicted energy bandgap of $\text{Ge}_{1-x}\text{Sn}_x$ without C is also shown for reference [2].